Applied Acoustics 242 (2026) 111087

Contents lists available at ScienceDirect

Applied Acoustics

journal homepage: www.elsevier.com/locate/apacoust

Active noise control in a tractor cabin: implementation challenges and experimental testing in driving conditions

Francesco Mori [a,*], Andrea Santoni [a], Cristina Marescotti [a], Patrizio Fausti [a], Francesco Pompoli [a], Christian Preti [b], Pietro Nataletti [c], Paolo Bonfiglio [d]

[a] Department of Engineering, University of Ferrara, via G. Saragat 1, 44122 Ferrara, Italy
[b] CNR-STEMS, Strada Provinciale 23 del Colle del Sestriere, n.18, 10060 Candiolo, Torino, Italy
[c] National Institute for Insurance against Accidents at Work (INAIL), 00078 Monte Porzio Catone, Rome, Italy
[d] Materiacustica s.r.l., via Ravera 15/A, 44122 Ferrara, Italy

HIGHLIGHTS

- A multi-channel active noise control system was implemented for a tractor cabin.
- ANC performance was evaluated under both static and driving conditions.
- An accelerometer on the engine was utilized as a reference sensor.
- ANC reduces the perceived loudness inside the cabin.

ARTICLE INFO

Keywords:
Active noise control
Multichannel systems
FXLMS
Tractor

ABSTRACT

Tractor drivers are often exposed to high levels of low-frequency noise for prolonged periods, leading to discomfort and, in some cases, hearing loss. A major contributor to the noise transmitted into the cabin is the tractor engine, which generates a series of harmonic components, predominantly in the low-frequency range (below 1000 Hz). Due to space limitations inside the tractor cabin and the necessity of transparent surfaces to ensure visibility, effective passive noise mitigation can hardly be implemented. Active noise control (ANC) represents a suitable and modern technique to attenuate unwanted noise. This paper presents an experimental evaluation of a multi-channel ANC system applied to a tractor cabin, aimed at reducing the driver's exposure to noise generated by a four-cylinder engine. The system implements the well-established filtered-X least mean squares (FXLMS) algorithm in a multi-channel feedforward configuration to generate control signals, employing an accelerometer mounted on the engine as a reference sensor. Initial tests were carried out under stationary conditions, by varying the engine's revolutions per minute. Subsequent tests were performed under different driving conditions on an asphalt ring track, varying gear, range, and crankshaft rotational speed. The results demonstrate the effectiveness of the ANC system in reducing engine-related noise components between 80 Hz and 500 Hz. The low-frequency limit is imposed by the frequency response of the control loudspeakers. To enhance algorithm efficiency, a digital low-pass filter is applied to prevent instability introduced by high frequencies.

1. Introduction

In recent decades, acoustic comfort and prevention of hearing damage have become relevant in different working contexts. The most recent reports published by INAIL (the Italian National Institute for Insurance against Industrial Injuries) in 2018 and 2022 estimated an average of 4600 hearing loss accident reports per year in Italy, from 2011 to 2019, in a professional context. Among the various worker categories considered in these reports, agriculturists are particularly exposed to loud noise for prolonged periods. One of the most significant noise sources that affect the driver in the tractor cabin is the engine. It generates loud low-frequency harmonics, mainly in the range between 20 Hz and 1000 Hz, propagating into the cabin through both structure-borne and air-borne paths. The characteristics of the generated noise depend on

* Corresponding author.
Email address: francesco.mori@unife.it (F. Mori).

https://doi.org/10.1016/j.apacoust.2025.111087
Received 20 December 2024; Received in revised form 12 September 2025; Accepted 13 September 2025
Available online 22 September 2025

the type of engine and its workload condition [1,2]. Other important noise sources [3] include the exhaust, cooling fan, and plough or harrow (depending on the type of work), as well as rolling tyres when operating on hard surfaces. The noise perceived inside the cabin typically consists of a series of low-frequency harmonics, mainly caused by the direct vibrational excitation of the cabin itself, which radiates noise to the receiver [4]. Unlike cars or other road vehicles, where engine harmonics are typically masked by rolling and wind-borne noise at cruising speeds, these harmonics dominate the complex acoustic field inside the tractor cabin. Many of the mentioned noise sources are attenuated by the presence of the tractor cabin, particularly in the medium-high frequency range [5,6]. However, improving noise insulation is a cumbersome task: the limited space inside the cabin and the necessity to ensure visibility through transparent surfaces, restrict the placement of absorbing materials or insulation packages. To reduce exposure to noise, headphones or, in general terms, personal protective equipment can be used for localised noise control [7]. However, prolonged use of these devices often causes discomfort for many people. Furthermore, hearing protection devices typically show limited performance in the frequency range below 500 Hz [8]. In this framework, an active noise control (ANC) system offers a viable alternative solution to attenuate noise in a lower frequency range [9]. In the broadest sense of the term, an ANC system is an electro-acoustic device, computing and generating by means of a control loudspeaker, an "anti-noise" signal with equal amplitude and opposite phase with respect to an undesired noise. The superposition of these two signals makes them cancel each other in a region of space denominated "zone of quiet". The signal driving the control source can be computed with different techniques, depending on the configuration of the ANC system and the algorithm implemented [10].

Although ANC systems have been extensively investigated in the automotive field [11–13] and some commercial solutions are present on the market [14,15], ANC systems for tractors have not yet been commercialized and related research remains limited. The first known study found in the literature regarding the application of an ANC system to tractors was published in 1995 by Yoshida [16]. The author carried out a study on tractors without a cabin, analysing the effect of both a feedforward system, with one reference microphone, and a feedback system. Both configurations consisted of two control loudspeakers and one error microphone. Subsequent studies by Pochi et al. [17], tested a feedback system with two error microphones and two control loudspeakers. Further research explored ANC systems applied to an agricultural machine equipped with a cabin. For instance, Carme et al. [18] investigated a feedforward ANC system, with one reference microphone behind the driver's seat, on a loader machine. Gulyas et al. [19] analysed multiple configurations on a harvester machine, studying the performance of a feedforward system with a reference microphone outside the cabin, a feedforward system with feedback compensation and a reference microphone inside the cabin, and a feedback system. Sun et al. studied a hybrid feedback-feedforward system for an excavator, measuring the engine speed as a reference signal [20]. All these configurations employed two control loudspeakers and two error microphones. Other authors [21,22] concentrated their studies on ANC systems for tractors with a cabin, developing a feedback system with two control sources and two error microphones. In all the cases previously cited, an algorithm based on the least mean squares (LMS) method was implemented. Moreover, experimental measurements were performed on a tractor without motion for a stationary number of revolutions per minute of the engine. To simulate workload conditions, Fanigliulo et al. employed a dynamometric brake to assess ANC performance under engine stress [21].

This article investigates the applicability of an ANC system inside a tractor cabin to reduce the driver's exposure to noise. The proposed ANC system features a feedforward configuration with two control sources and two error microphones, one for each ear. This study also explores the use of an accelerometer as a reference sensor. Such a sensor has been successfully employed in ANC systems on several vehicles, including mining trucks, high-speed boat wheelhouses, and locomotive cabins, to suppress several harmonic components in the sensed noise spectra [23,24]. Accelerometers have also been used in the automotive field, to suppress structure-borne noise typically coming from tyre-road interaction [25–30] and window vibration [31]. However, the use of accelerometers has not yet been examined in the literature for the case of tractors. Unlike previous studies focused only on static conditions, this research evaluates ANC performance in both static and driving scenarios, varying gear, range, and crankshaft rotational speed. The ANC system implements the classical filtered-X least mean squares (FXLMS) algorithm with offline estimation of secondary paths [32], extended to the case of a multi-channel ANC system and adapted to mitigate instability issues.

This paper is structured in five sections. The next section describes the analysed case study, the experimental setup employed during the tests, and the scheme of the ANC system. In Section 3 the noise perceived by the driver and its correlation with the reference sensor are analysed. Section 4 illustrates and discusses the results obtained in both static and dynamic tests, evidencing the effect of each parameter variation. Finally, Section 5 summarises the main findings of this research and the possible future developments to enhance the robustness and performance of the ANC system for tractors.

2. Methodology

2.1. Case study description

Experimental tests for both cabin noise analysis and evaluation of ANC system performance were carried out on a New Holland T 4050 tractor equipped with an enclosed cabin (Fig. 1(a)). The tractor has a four-cylinder inline engine with a firing order of 1–3–4–2, operating on a four-stroke diesel cycle. Thus, the two pairs of cylinders are mounted on the crankshaft with a 180° phase offset, and a firing event occurs every two cycles of each cylinder. Moreover, the engine is characterised by a power of 71 kW (97 hp) and a cubic capacity of 4500 cc. The transmission consists of four ranges and four gears, providing a total of 16 gear ratios. Due to the periodic motion of the cylinders, the vibrational spectrum generated by the engine comprises a series of narrowband components, with a fundamental frequency and its harmonics expressed by the following formula:

$$f_n(Hz) = n\frac{rpm}{60}, \quad n = 0.5, 1, 1.5, \dots \tag{1}$$

where n denotes the engine order (comprising the half-orders) and rpm is the engine speed in revolutions per minute. Among these components, combustion orders can be identified as the frequencies corresponding to even multiples of engine orders, due to the four-cylinder, four-stroke configuration.

Engine excitation can reach the driver's ears through two paths: an air-borne path, where the noise propagates through the air, and a structure-borne path, where vibrations directly excite the cabin structure through its suspension system. To distinguish the individual contributions to the overall noise perceived by the driver, a Transfer Path Analysis (TPA) should be carried out. However, such an expensive study, both in terms of time and resources, goes beyond the scope of this work. Instead, simpler analyses of the noise perceived inside the cabin and its coherence with a reference signal are illustrated in Section 3. ANC performance was evaluated under both stationary and dynamic conditions. In the stationary case, the tractor engine was operated at constant rpm while the vehicle remained motionless. This allowed for controlled conditions in which engine noise was the dominant source. For dynamic conditions, tests were carried out on a 1 km-long asphalt ring track at the National Research Council (CNR) in Turin (Fig. 1(b) and Fig. 1(c)). The tractor was driven at different engine speeds and with different gear and range combinations, corresponding to different travel speeds. The dynamic condition introduced additional noise sources, such as tyre rolling

Fig. 1. Photographs of the case study. a) New Holland T 4050 tractor, b) satellite view of the test track, c) track view from the tractor cabin.

noise and transmission noise, along with variations in engine load. It is important to note that these two testing conditions are not directly comparable. The driving condition can modify existing noise sources (e.g., due to engine workload) and introduce new ones (e.g., tyre and transmission noise), creating a more complex acoustic field.

2.2. Description of the active noise control system

The feedforward ANC system implemented in these tests is schematically represented in Fig. 2. Two 1/2” PCB 377B02 microphones, acting as error sensors, are located inside the cabin, on a wooden board fixed to the seat, so that they are close to the driver’s ears. These microphones measure the error signals $e_i(n)$ $(i = 1, 2)$ that must be attenuated on the left and right sides of the driver’s head, respectively. Two control sources consist of two Avantone MixCubes Active loudspeakers, each equipped with an internal amplifier and a 5.25” driver. These are mounted inside the cabin on a shelf behind the seat, at the height of the driver’s shoulders. They generate the anti-noise signals $y_j(n)$ $(j = 1, 2)$ computed by the algorithm implemented in the control unit. Loudspeakers were chosen as the best trade-off between their size and their frequency response. While larger drivers would be required to achieve lower cut-on frequencies, spatial constraints within the cabin limited this choice. The selected devices provide a declared cut-on frequency of 100 Hz. In addition to the previous devices, a PCB 353B15 accelerometer is mounted outside the cabin, on a steel element rigidly fixed to the engine frame. This sensor acquires a reference signal $x(n)$ related to the vibration directly generated by the movement of the cylinders. The noise from the engine reaches the driver through the two types of primary paths mentioned in the previous section: the air-borne path $p_{i,A}$ $(i = 1, 2)$ and the structure-borne path $p_{i,S}$ $(i = 1, 2)$. Since the reference sensor is an accelerometer positioned outside the tractor cabin, it is protected against feedback signals propagating from the control sources. As a result, there is no necessity to model feedback paths in the algorithm. Therefore, the classical filtered-X least mean squares (FXLMS) algorithm, developed for a multi-channel system and accounting for the four secondary paths s_{ji} was adopted. This kind of algorithm is particularly effective in the presence of periodic signals, including tonal components and pseudo-random noise. Since engine noise contains harmonics at multiples of the crankshaft rotational frequency, the FXLMS algorithm is well suited for the cancellation of these components.

This system operates as follows. After acquiring a sample of the error signals $e_1(n)$ and $e_2(n)$ and of the reference signal $x(n)$, the control unit computes the filtered reference signals as:

$$x'_{ji}(n) = \sum_{m=0}^{M-1} s'_{ji,m}(n)x(n-m), \tag{2}$$

where M is the length of the finite impulse response (FIR) filters estimating the secondary paths $s'_{ji} = [s'_{ji,0}\ s'_{ji,1}\ \dots\ s'_{ji,M-1}]$. The adaptive filters $w_j(n) = [w_{j,0}(n)\ w_{j,1}(n)\ \dots\ w_{j,K-1}(n)]$ of length K are updated according to the following equation, deriving from the minimization of the total energy sensed by the two error microphones:

$$w_{j,k}(n+1) = w_{j,k}(n) - \mu \sum_{i=1}^{2} e_i(n)x'_{ji}(n-k) \quad k = 0, 1, \dots, K-1, \tag{3}$$

where μ is the step-size parameter, regulating both the convergence rate and algorithm stability. Finally, the outputs driving the two control sources are evaluated as:

$$y_j(n) = \sum_{k=0}^{K-1} w_{j,k}(n)x(n-k). \tag{4}$$

This procedure is repeated for any generic instant n. In this implementation, a filter length of 1024 elements was used for both the secondary paths and the adaptive filters. The step-size parameter μ was adjusted according to engine speed. Secondary paths were identified offline using the white noise excitation procedure described in [9], where each control source is driven individually and the corresponding impulse response is estimated using the LMS algorithm.

The entire system is driven by a National Instruments real-time target (cRio 9063) with FPGA (Field Programmable Gate Array). Input and output signals are sampled at a rate of 6400 Hz and data are processed in a deterministic way using the aforementioned algorithm. To prevent excessive output voltage in the case of instability, the control unit limits the control signal amplitude to 1 V. Furthermore, to reduce sensitivity to secondary path variations, especially during motion, a fourth-order digital Butterworth low-pass filter with a cut-off frequency of 600 Hz was applied to the reference signal. This prevents the algorithm from processing higher-frequency components that are more susceptible to environmental variability, for instance related to the relative oscillation between loudspeakers and error microphones.

3. Cabin noise analysis

3.1. Static conditions

Noise analysis under motionless conditions was carried out at three different engine speeds, referred to as 840 rpm (minimum), 1520 rpm (medium), and 2520 rpm (maximum) in the following discussion. The analysis focuses on a frequency range up to 500 Hz, where most of engine harmonics are concentrated. The signal processing of the ANC algorithm is limited by the digital low-pass filter with a cut-off frequency of 600 Hz.

Fig. 3(a) shows the sound pressure level (SPL) spectra sensed inside the cabin by the right (red) and left (blue) error microphones at 840 rpm. Additionally, Fig. 3(b) displays the coherence function value, computed at the frequencies of the engine harmonics, between the external sensor and the error microphones. At this minimum engine speed, the highest tonal components are concentrated in the range below 120 Hz, where coherence between the internal microphones and the reference accelerometer assumes high values up to order x8. However, as will be discussed in Section 4, despite the high energy content characterising this frequency range, the effectiveness of the ANC system is limited by the frequency response of the loudspeakers employed in the cabin setup, especially below 80 Hz. At higher frequencies, the coherence between the reference accelerometer and the error microphones fluctuates. While certain frequencies show a high correlation, such as those associated with engine orders x18, x20.5, x24, and x26, others exhibit low coherence values (e.g., at orders x9.5, x10.5, x13, and x27.5). In general, tonal components become less significant in the spectrum

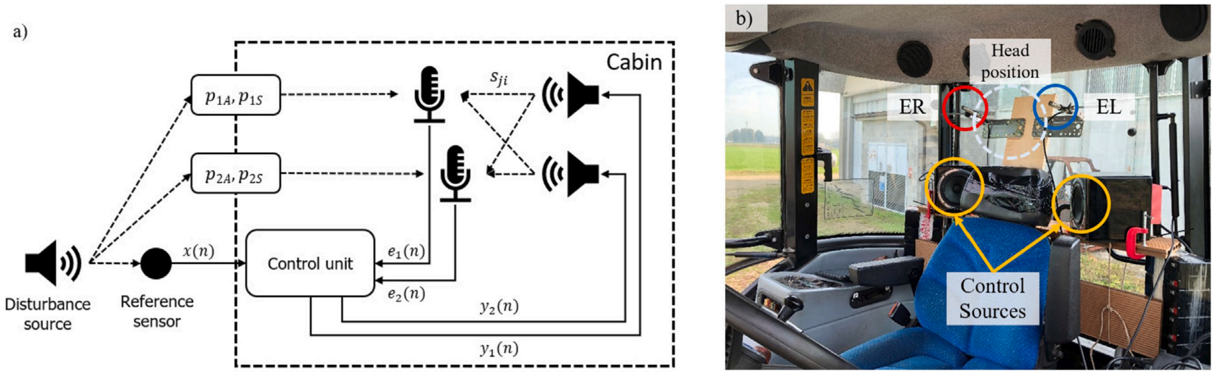

Fig. 2. a) Scheme of the feedforward ANC system, b) ANC setup inside the cabin.

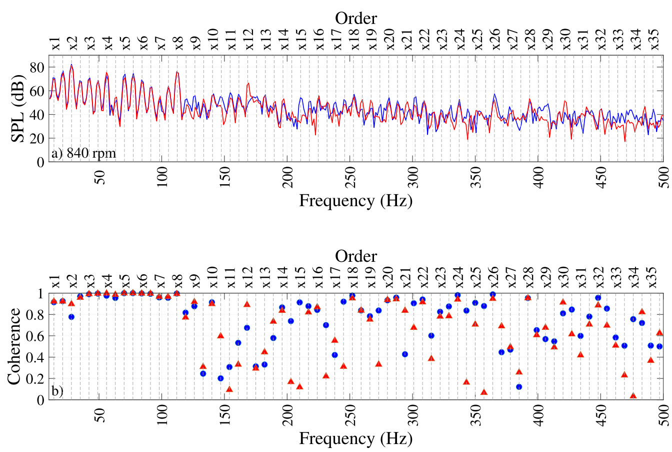

Fig. 3. a) Sound pressure level spectra inside the tractor cabin at 840 rpm. b) Coherence of the engine harmonics between the reference sensor and the microphones inside the cabin (left side in blue and right side in red).

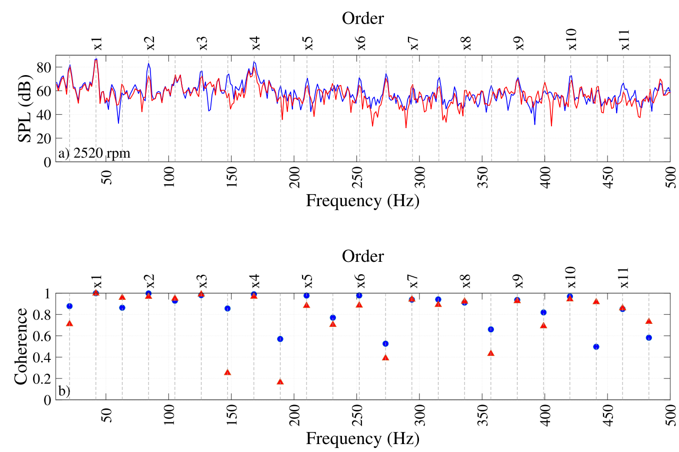

Fig. 5. a) Sound pressure level spectra inside the tractor cabin at 2520 rpm. b) Coherence of the engine harmonics between the reference sensor and the microphones inside the cabin (left side in blue and right side in red).

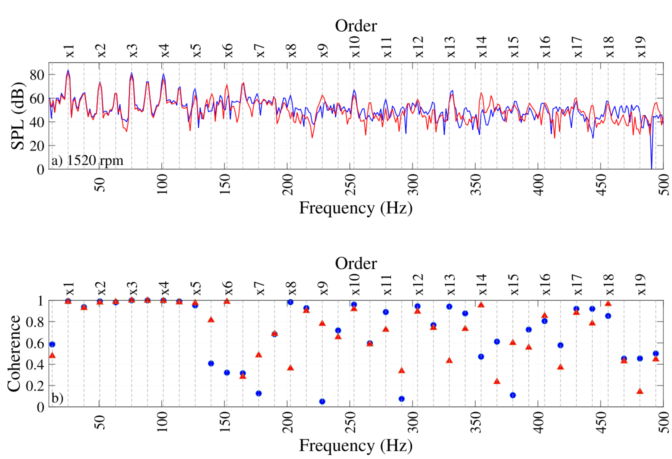

Fig. 4. a) Sound pressure level spectra inside the tractor cabin at 1520 rpm. b) Coherence of the engine harmonics between the reference sensor and the microphones inside the cabin (left side in blue and right side in red).

above 200 Hz, as broadband noise becomes more dominant in the SPL spectrum.

Similar conclusions can be drawn for the intermediate case at 1520 rpm, shown in Fig. 4. The most relevant components, exhibiting the largest magnitude, appear up to 165 Hz (between orders x1 and x6.5). In addition, higher-frequency peaks with larger amplitudes are found at 253 Hz, 329 Hz, and 355 Hz, associated with engine orders x10, x13, and x14. The coherence between the two sensors is high (> 0.9) for components up to order x5 and for certain even harmonics, associated with the combustion orders (e.g., x10 and x12).

Finally, Fig. 5(a) and Fig. 5(b) report the spectra and coherence at the maximum engine speed of 2520 rpm. The coherence between the reference and error sensors increases with engine speed. Compared to the previous conditions, a generally higher coherence is observed, with values exceeding 0.8, except at a few half-orders. However, in this condition, tonal components become less distinguishable due to the increased broadband noise. This could be due to the high excitation provided by the engine on both the mechanical parts and the cabin, efficiently radiating noise in a broader frequency range compared to lower engine speeds.

3.1.1. Loudness under static conditions

To gain a better understanding of the driver's perception of noise inside the tractor cabin, the specific loudness was evaluated according to Zwicker's method described in ISO 532–1:2017. The results for different engine speeds under static conditions are shown in Fig. 6. As illustrated, the main contributions to the overall perceived loudness are concentrated in the frequency range between 100 Hz and 300 Hz. However, relevant contributions can extend up to 500 Hz for high engine speeds, as can be noticed on the right side at 2520 rpm. Based on this observation, the loudspeaker frequency response and the cut-off frequency of

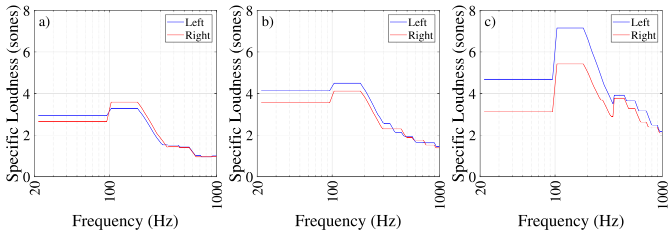

Fig. 6. Specific Loudness sensed by the error microphones under static conditions at a) 840 rpm, b) 1520 rpm, and c) 2520 rpm.

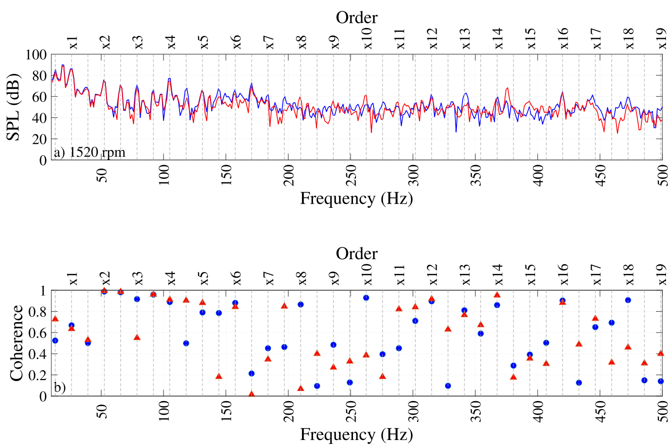

Fig. 7. a) Sound pressure level spectra inside the tractor cabin at 1520 rpm in the driving condition (gear 2, range 2). b) Coherence of the engine harmonics between the reference sensor and the microphones inside the cabin (left side in blue and right side in red).

the digital low-pass filter were considered acceptable for the development of the ANC system. In addition, comparing the three regimes, it can be observed that the specific loudness in that frequency range increases with the engine speed and the highest peak shifts from the right to the left side of the cabin.

3.2. Dynamic conditions

Similar to the static case, the noise analysis under driving conditions was performed by varying gear, range, and engine speed. As the tractor could not be operated at the same minimum rpm as in static conditions, three different nominal values of engine speed were defined: 1520 rpm, 2100 rpm and 2520 rpm.

Fig. 7 illustrates the results of the noise analysis carried out at 1520 rpm (gear 2 and range 2). Consistent with the results observed under motionless conditions, noise spectra inside the cabin are dominated by harmonic components associated with engine orders, particularly in the frequency range up to approximately 165 Hz (from order x1 to x6.5). On average, lower coherence is observed compared to motionless conditions. This reduction is likely due to additional noise sources introduced below 30 Hz and associated with the rolling effect of the tyres on the asphalt during movement. However, within the frequency range from 80 Hz to 165 Hz, high coherence is found between the reference accelerometer and the error microphones inside the cabin, except for engine order x3 on the left side, as well as half-orders x4.5 on the right side, x5.5 on the left side, and x6.5 on both sides.

Fig. 8 shows the SPL spectra and their coherence with the reference accelerometer for the driving condition at 2100 rpm. Fig. 8(a) highlights the highest magnitude at frequencies below 30 Hz, attributed to rolling noise generated by tyre-road interaction. These noise components are unrelated to the engine, as demonstrated by the low coherence

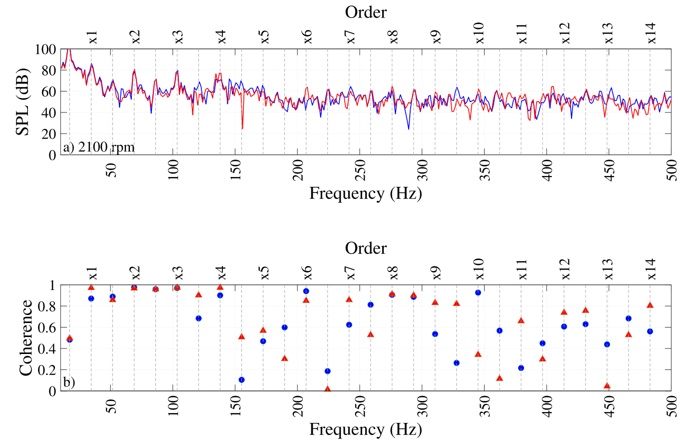

Fig. 8. a) Sound pressure level spectra inside the tractor cabin at 2100 rpm in the driving condition (gear 2, range 2). b) Coherence of the engine harmonics between the reference sensor and the microphones inside the cabin (left side in blue and right side in red).

shown in Fig. 8(b) in this frequency range. Engine-related components are significant up to 130 Hz, spanning from order x1 to order x4, where the spectra are characterised by prominent peaks and high coherence.

Similar conclusions can be drawn for the driving conditions at the highest engine speed, 2520 rpm, as shown in Fig. 9. The highest amplitude is found below 30 Hz, attributed to components associated with rolling noise. The main engine harmonic components are observed up to order x4 and between orders x6 and x7, characterised by prominent peaks and a coherence of 0.8 or higher in some cases.

Finally, the effect of different gears and ranges is analysed, considering a constant engine speed of 1520 rpm. The influence of the gear variation on the SPL spectra is negligible, while increasing the range affected the amplitude only below 70 Hz, which lies outside the effective range of the ANC system. However, changes in gear and range affected the coherence between the reference accelerometer and the error microphones. Fig. 10 shows the coherence between the accelerometer and the left microphone for different ranges (and, thus, different velocities), maintaining the same engine speed (1520 rpm) and the gear fixed to 2. In general terms, the increment of the range provides a reduction of the coherence on the main peaks, in particular between orders x3.5 and x6. This fact suggests that reduced engine workload and higher tractor speed lead to lower coherence between the external sensor and the noise signals sensed inside the cabin, potentially reducing the effectiveness of the ANC system. Similar considerations apply to gear variation.

3.2.1. Loudness under dynamic conditions

As in the static conditions, specific loudness was also evaluated under dynamic conditions, maintaining the same transmission ratio with gear 2 and range 2. The results for the three investigated engine speeds are presented in Fig. 11. Similarly to the previous case, the most significant contributions to perceived loudness are concentrated in the range between 100 Hz and 300 Hz. The magnitude of the specific loudness within this range increases with engine speed. Additionally, at higher speeds, relevant contributions extend up to 400 Hz, where the specific loudness reaches values comparable to those found in the range below 100 Hz. These findings, obtained under both static and dynamic conditions, suggest that the ANC system should primarily focus on the frequency range between 100 Hz and 300 Hz, with a possible extension up to 500 Hz depending on the operating condition. Targeting this frequency range can effectively reduce the driver's perception of noise inside the tractor cabin.

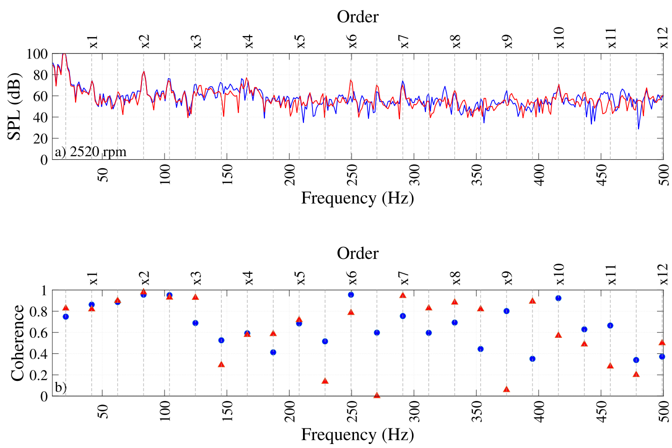

Fig. 9. a) Sound pressure level spectra inside the tractor cabin at 2520 rpm in the driving condition (gear 2, range 2). b) Coherence of the engine harmonics between the reference sensor and the microphones inside the cabin (left side in blue and right side in red).

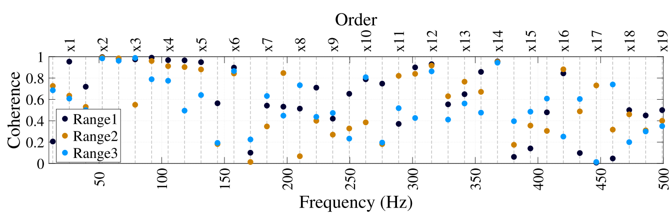

Fig. 10. Coherence between the reference sensor and the left microphone inside the cabin, varying the range in the driving condition (maintaining gear 2, 1520 rpm).

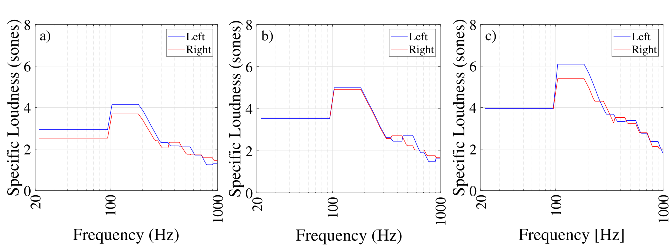

Fig. 11. Specific Loudness sensed by the error microphones under dynamic conditions at a) 1520 rpm, b) 2100 rpm, and c) 2520 rpm.

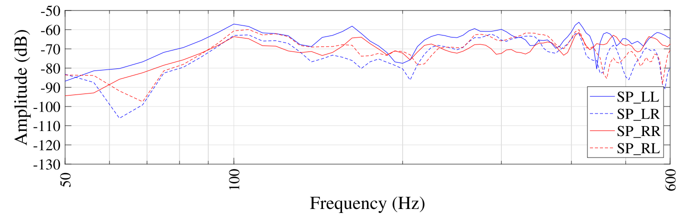

Fig. 12. The secondary paths (SP): the first letter L/R indicates the left/right control source, the second letter L/R refers to the left/right error microphone.

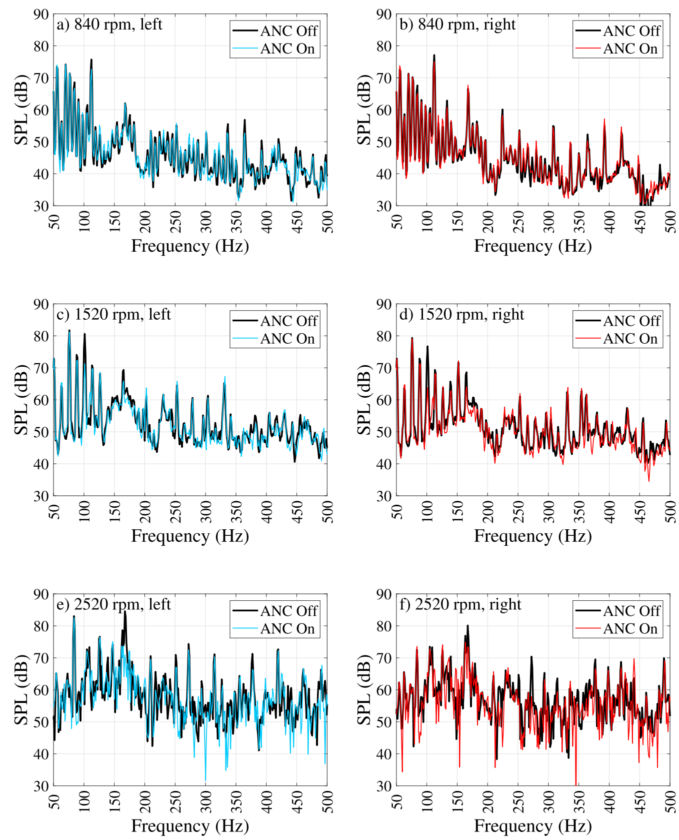

Fig. 13. Sound pressure level with ANC turned off and on for the analysed engine speeds under static conditions: a) and b) 840 rpm, c) and d) 1520 rpm, e) and f) 2520 rpm.

4. Evaluation of the ANC performance

4.1. Estimation of the secondary paths

The measurements of the secondary paths were carried out under the same conditions as the experimental test, with a driver seated on the tractor seat and a second person located to the left of the driver inside the cabin, conducting the acoustic measurements. The results of the offline estimation of the secondary paths are illustrated in Fig. 12. Below approximately 80 Hz, the control loudspeakers exhibit limited output power, making them incapable of radiating sufficient acoustic energy in the low-frequency range. This limitation defines the lower bound of the frequency range for the ANC system. From the spectra of both the direct and cross paths, nodal positions of the error microphones can be identified at certain frequencies where the amplitude decreases. At these frequencies, the efficiency of the ANC system in attenuating disturbing noise is reduced because of the influence of cabin cavity modes. Furthermore, the spectra in Fig. 12 show an asymmetry in the sound field at the two error microphone positions. The direct secondary path from the left loudspeaker to the left error microphone (SP_LL) exhibits a larger amplitude compared to the opposite side (SP_RR), probably due to the non-perfectly symmetric orientation of the loudspeakers and the presence of the person seated on the left side inside the cabin. Conversely, the cross paths (SP_LR and SP_RL) are similar to each other and comparable to the direct paths (SP_LL and SP_RR) up to 400 Hz. Above this frequency, the direct paths show a larger amplitude with respect to the cross paths.

4.2. Results under static conditions

This section presents the performance of the ANC system under static conditions, by comparing the sound pressure level (SPL) spectra recorded with the ANC system turned off and after 20 s of activation. Additionally, the attenuation—defined as the difference in amplitude between the two conditions—is reported for selected harmonic components and for the overall noise level. The SPL spectra obtained at the three nominal engine speeds under motionless conditions (840 rpm,

Table 1
Attenuation (dB) measured under static conditions for different engine speeds for some relevant harmonics and overall noise levels. Data are indicated as: Left attenuation, right attenuation (order, frequency).

rpm	Harmonic 1	Harmonic 2	Harmonic 3	Overall (dB)	Overall (dB(A))
840 rpm	3.0, 2.2 (x8, 112 Hz)	3.1, 0.0 (x24, 336 Hz)	4.1, 2.0 (x26, 364 Hz)	1.6, 1.7	1.1, 1.1
1520 rpm	3.6, 3.5 (x3.5, 88 Hz)	10.5, 13.3 (x4, 101 Hz)	4.0, 5.1 (x6.5, 165 Hz)	1.8, 1.6	0.6, 0.9
2520 rpm	13.7, 6.7 (x4, 168 Hz)	3.9, 7.4 (x6, 252 Hz)	1.9, 12.5 (x6.5, 273 Hz)	2.6, 1.5	2.0, 0.6

1520 rpm, and 2520 rpm) are shown in Fig. 13. In general, the ANC system's performance at each harmonic component depends on multiple factors: the coherence between the reference and error signals (as discussed in the previous section), the signal amplitude, and the magnitude of the four secondary paths. Each harmonic component should therefore be evaluated individually, considering the influence of these parameters.

At all tested engine speeds, the ANC system demonstrates limited attenuation at low frequencies, particularly below 80 Hz, due to the restricted low-frequency response of the control loudspeakers, which are unable to supply sufficient acoustic power in this range. However, as also observed in the specific loudness analysis, these low-frequency contributions have a lower impact on human perception of noise inside the cabin. At minimum engine speed (840 rpm), attenuation is distributed across various harmonic components, with a peak reduction of 6 dB at the right error microphone for engine order x34.5 (483 Hz), as shown in Fig. 13(b). At 1520 rpm (Fig. 13(c) and Fig. 13(d)), the maximum attenuation occurs at the second combustion order (x4, 101 Hz), which is the first harmonic that falls within the frequency range where the loudspeakers operate efficiently. This harmonic is characterised by both high amplitude and high coherence. Finally, at 2520 rpm (Fig. 13(e) and Fig. 13(f)), the most significant attenuation is again observed at order x4 (168 Hz), corresponding to the second combustion order and exhibiting high coherence and amplitude. Minor attenuation is observed on higher-order harmonics, which generally have lower amplitudes.

Table 1 summarises the attenuation measured for some of the most relevant components and for the overall noise level, evaluated within the 80 Hz - 500 Hz frequency range, where the ANC system is designed to be more effective. The table reports both linear and A-weighted overall attenuation for each engine speed. The SPL was measured using the error microphones involved in the ANC system, which had been previously calibrated and positioned close to the driver's ears. The linear overall attenuation progressively increases with engine speed. This can be correlated to a rise in the average coherence, as well as to the first harmonics falling into the range above the loudspeaker cut-on frequency. In contrast, the A-weighted attenuation does not exhibit a clear trend with engine speed. In general, A-weighted attenuation values are lower than the corresponding linear values, since the ANC system primarily targets the low-frequency range, which is less emphasised by A-weighting.

The effect of the ANC system on overall loudness is illustrated in Fig. 14. For engine speeds of 1520 rpm and 2520 rpm, the loudness is reduced by up to 2 sones on the left side. This is consistent with the greater overall attenuation observed in the linear SPL level on that side. In contrast, the right side experiences lower noise reduction. Although the absolute reduction in overall noise level is modest, loudness variation suggests that the ANC system can produce a perceptible change in the acoustic environment perceived by the driver inside the cabin.

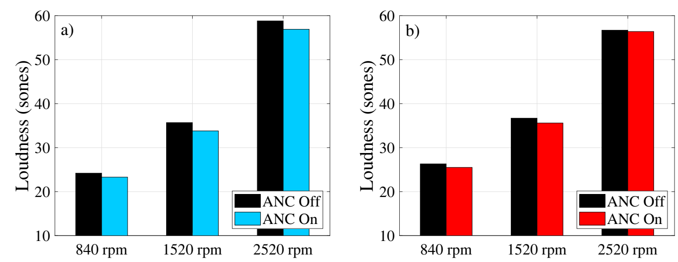

Fig. 14. Loudness with ANC turned off and on for the analysed engine speeds under static conditions: a) left side, b) right side.

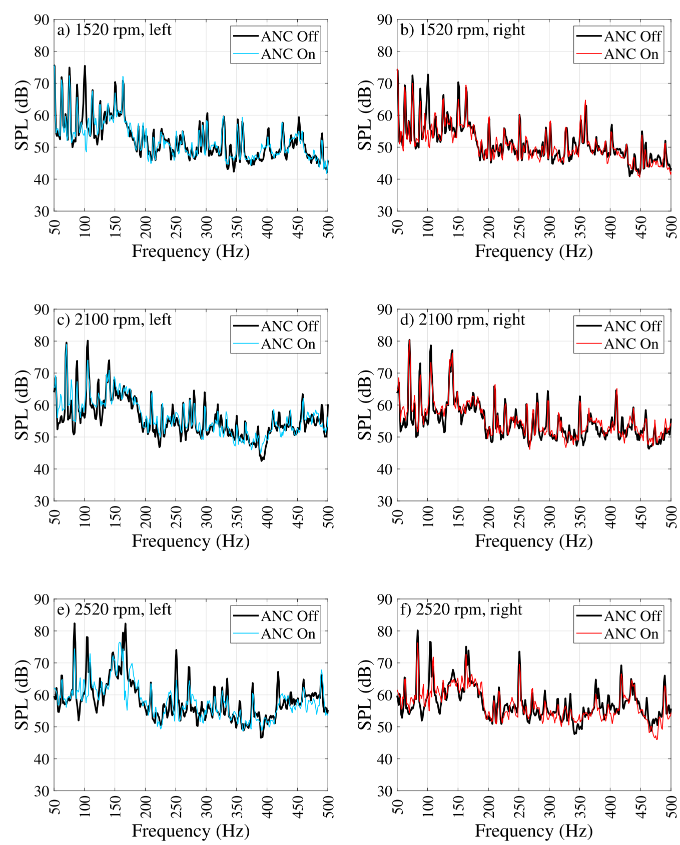

Fig. 15. Sound pressure level with ANC turned off and on for the analysed engine speeds under dynamic conditions: a) and b) 1520 rpm, c) and d) 2100 rpm, e) and f) 2520 rpm.

4.3. Results under dynamic conditions

The performance of the ANC system was also evaluated under dynamic conditions, driving at constant speed for various combinations of gear, range, and engine speed (rpm). Attenuation was assessed using the same definition adopted for the static condition, along the two straight segments of the test track (each approximately 300 m long) to minimize asymmetric effects caused by road curvature. To investigate the influence of engine speed on ANC effectiveness, SPL spectra were analysed at a fixed transmission ratio (range 2, gear 2) for different nominal rotational speeds: 1520, 2100, and 2520 rpm. The corresponding results are reported in Fig. 15. For the minimum tested regime (Fig. 15(a) and

Table 2
Attenuation (dB) measured under dynamic conditions (range 2, gear 2) for different engine speeds for some relevant harmonics and overall noise levels. Data are indicated as: Left attenuation, right attenuation (order, frequency).

rpm	Harmonic 1	Harmonic 2	Harmonic 3	Overall (dB)	Overall (dB(A))
1520 rpm	20.1, 17.4 (x4, 101 Hz)	3.4, 5.3 (x6, 152 Hz)	5.1, 2.6 (x16, 405 Hz)	1.1, 1.3	0.0, 0.1
2100 rpm	6.5, 3.6 (x2.5, 87 Hz)	6.1, 5.3 (x3, 105 Hz)	4.3, 3.0 (x8.5, 297 Hz)	1.3, 0.8	0.9, −0.6
2520 rpm	8.0, 4.0 (x2, 84 Hz)	21.1, 8,6 (x4, 168 Hz)	9.5, 4.0 (x6, 252 Hz)	1.4, 2.2	0.4, 1.4

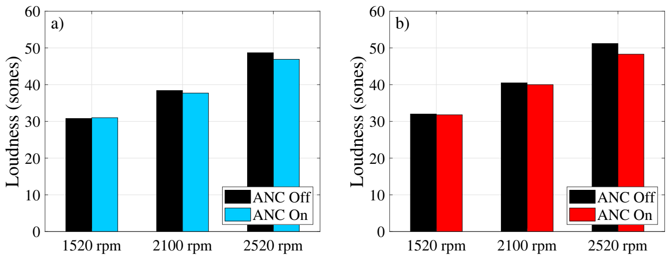

Fig. 16. Loudness with ANC turned off and on for the analysed engine speeds under dynamic conditions: a) left side, b) right side.

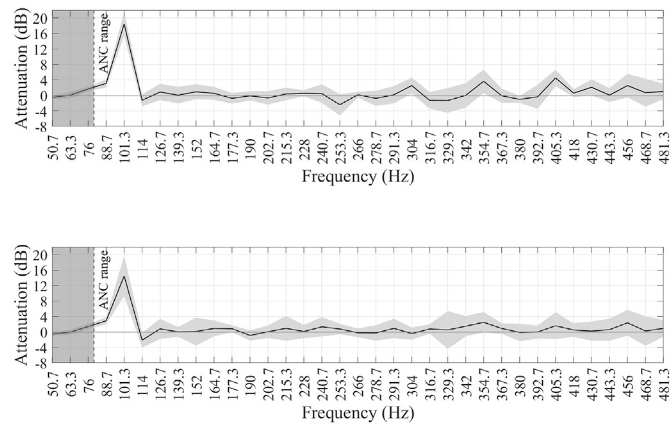

Fig. 17. Average attenuation in the driving condition at 1520 rpm: a) left side, b) right side.

Fig. 15(b)), the highest attenuation is observed at the second combustion order (order x4, 101 Hz), consistent with the motionless tests, but with a higher value compared to the previous study.

At the nominal value of 2100 rpm (Fig. 15(c) and Fig. 15(d)), the attenuation decreases and spreads across the frequency spectrum, starting from around 80 Hz. Finally, Fig. 15(e) and Fig. 15(f) illustrate the case at 2520 rpm, where, the ANC system works efficiently mainly on the even multiples of the combustion frequency (for instance, orders x2, x4, x8) as well as other components characterised by high coherence.

Table 2 reports the overall attenuation for each engine speed, computed as both linear and A-weighted sums. The results highlight an improvement in ANC performance with increasing engine speed. Nevertheless, the highest attenuation for an individual harmonic is observed at the lowest tested speed (1520 rpm), specifically at 104 Hz (order x4). Compared to the static condition, overall attenuation is slightly reduced, likely due to additional noise sources introduced during driving, such as rolling noise. Moreover, the A-weighted attenuation remains limited because the ANC system primarily targets low-frequency components.

To better assess the noise perceived inside the cabin, overall loudness values are presented in Fig. 16. Similar to the static condition, the overall loudness increases with the engine speed. Simultaneously, loudness reduction increases with engine speed, reaching a maximum of 3 sones on the right side and 2 sones on the left side at 2520 rpm, improving the acoustic comfort in the worst situation.

Finally, the influence of different transmission combinations, in terms of gear and range, on the attenuation produced by the ANC is analysed considering a fixed engine speed at 1520 rpm. Fig. 17 shows the attenuation obtained for all tested combinations. The average behaviour for the specified crankshaft rotational speed is indicated by a solid black line, while the standard deviation is depicted as a shaded grey area. The results reveal that ANC performance does not strongly depend on the selected transmission ratio. As the loudspeaker cut-on frequency is approached, attenuation increases, peaking at order x4 (104 Hz). Beyond this frequency, attenuation is generally limited across all configurations, with a maximum of 8 dB observed for orders x14 and x16 on the left side. Although similar attenuation spectra were obtained across different transmission conditions, significant variability was observed in terms of overall attenuation. Table 3 summarises the overall attenuation evaluated as both linear and A-weighted sums in the frequency range from 80 Hz to 500 Hz. It is evident that the ANC system performs better

Table 3
Overall attenuation measured for different combinations of gears and ranges (1520 rpm).

Combination	(dB)		(dB(A))	
	Left	Right	Left	Right
Gear 1 - Range 2	1.2	1.0	0.2	0.2
Gear 2 - Range 2	1.1	1.3	0.0	0.1
Gear 3 - Range 2	−0.2	0.8	−0.1	−0.1
Gear 2 - Range 1	3.7	4.1	1.4	1.5
Gear 2 - Range 3	1.7	1.2	0.9	0.9
Average	1.5	1.7	0.5	0.5

when range 1 is adopted. Furthermore, the attenuation achieved with the combination of range 1 and gear 2 outperforms that of gear 1 and range 2. A similar trend is observed for range 3 and gear 2 compared to range 2 and gear 3, although the difference is smaller. Since ANC primarily affects low-frequency components such as order x4 (104 Hz), A-weighted attenuation values remain lower than their linear counterparts, reducing the perceptual significance of these differences among transmission ratios.

5. Conclusions

This article aims at evaluating the applicability of an ANC system in a tractor cabin to reduce driver's exposure to noise. To address a gap in the literature, which is largely focused on motionless tests, the performance of a multi-channel feedforward ANC system was investigated, under both static and various driving conditions. Unlike most prior studies on tractors employing reference microphones, the tested system used an accelerometer as a reference sensor.

The analysis of noise perceived inside the tractor cabin revealed that it was characterised by a series of harmonics generated by the engine, with the highest contributions mainly located in the frequency range below 500 Hz. These components exhibited a high coherence between the noise sensed by the microphones inside the cabin and the signal of the accelerometer, making them suitable targets for feedforward control.

Given the limitations imposed by the frequency response of the control loudspeakers and the digital low-pass filter implemented in the ANC algorithm, the analysis of the ANC performance focused on the harmonics present in the frequency range between 80 Hz and 500 Hz. Although this range does not significantly affect the overall A-weighted noise level, whose main contributions extend up to 2000 Hz, low-frequency ANC remains relevant for the improvement of noise perception, as suggested by loudness attenuation. In this framework, high-frequency components can be mitigated using passive treatments to obtain a larger reduction of the A-weighted noise level, while ANC can complement them by targeting low-frequency tonal noise, which strongly influences perceived driver fatigue and loss of concentration.

The results indicated that coherence played a key role in determining ANC performance. The frequency response of the loudspeakers represented the main limitation in extending the control bandwidth to lower frequencies, where the engine's strongest harmonics reside. However, spatial constraints in the cabin hindered the use of larger, more capable loudspeakers. Peak attenuation levels of 14 dB in static conditions and 22 dB in dynamic conditions were achieved for specific harmonics. Nevertheless, high attenuation at individual frequencies did not necessarily correspond to significant reductions in overall noise levels. Generally, motionless tests yielded better global performance than driving ones, where multiple variables, such as transmission ratio, engine speed, and workload, affected the acoustic field inside the cabin.

Future work will aim to extend the effective frequency range of the ANC system further into the low-frequency domain. This would allow control over more dominant tonal components currently beyond the capability of the installed loudspeakers. However, cabin space limitations remain a critical design constraint. As an alternative strategy, the use of vibrational actuators for radiation control of the cabin walls could be explored. Additionally, optimizing the number and location of reference sensors could help maximize the coherence between the signals inside the cabin and the external noise sources, thus improving the attenuation of high-amplitude components. Further improvements should also focus on enhancing the system's adaptability and robustness. In particular, implementing a normalized step-size algorithm [33–35] would allow for a complete automation of the ANC system, regardless of the engine speed. Furthermore, real-time secondary path estimation [36–38] could account for environmental changes, such as door openings and operator movements, thereby improving the system's flexibility. Finally, the ANC system should be tested during real-world agricultural operations, where the dominant noise sources may differ from those considered in the present study.

CRediT authorship contribution statement

Francesco Mori: Writing – original draft, Methodology. **Andrea Santoni:** Writing – review & editing, Data curation. **Cristina Marescotti:** Methodology, Data curation. **Patrizio Fausti:** Supervision, Project administration. **Francesco Pompoli:** Writing – review & editing, Supervision. **Christian Preti:** Validation, Investigation. **Pietro Nataletti:** Project administration, Funding acquisition. **Paolo Bonfiglio:** Methodology, Investigation.

Declaration of competing interests

The authors declare that they have no known competing financial interests or personal relationships that could have appeared to influence the work reported in this paper.

Acknowledgements

This work was supported by the BRIC 2022 ID-11 project from INAIL (National Institute for Insurance against Accidents at Work).

Data availability

Data will be made available upon request.

References

[1] Yadav PS, Gaikwad AA, Badgujar SY, Surkutwar YV, Karanth NV. Noise reduction on agricultural tractor. SAE technical paper. 2013. 2013–26–0103. https://doi.org/10.4271/2013-26-0103
[2] Dewangan KN, Prasanna Kumar GV, Tewari VK. Noise characteristics of tractors and health effect on farmers. Appl Acoust 2005;66(9):1049–62. https://doi.org/10.1016/j.apacoust.2005.01.002
[3] Ravindran V, Prakash B. Agricultural tractor noise control. SAE technical paper. 2013. 2013–01–2342. https://doi.org/10.4271/2013-01-2342
[4] Velioglu S, Yildiz A, Doganli M, Tandogan O. Interior noise analysis and prediction of a tractor cabin with emphasis on correlations with experimental data. SAE technical paper. 2013. 2013–01–1964. https://doi.org/10.4271/2013-01-1964
[5] Talamo JDC. Effects of cab noise environment on the hearing perception of agricultural tractor drivers. Appl Acoust 1979;12(2):125–37. https://doi.org/10.1016/0003-682X(79)90030-6
[6] Han HW, Im WH, Choi HJ, Cho SJ, Lee SD, Park YJ. Interior noise analysis and prediction of a tractor cabin with emphasis on correlations with experimental data. Sci Rep 2022;12:22038. https://doi.org/10.1038/s41598-022-26408-3
[7] Pessina D, Guerretti M. Effectiveness of hearing protection devices in the hazard reduction of noise from used tractor. J Agric Eng Res 2000;75(1):73–80. https://doi.org/10.1006/jaer.1999.0489
[8] Rudzyn B, Fisher M. Performance of personal active noise reduction devices. Appl Acoust 2012;73(11):1159–67. https://doi.org/10.1016/j.apacoust.2012.05.013
[9] Kuo SM, Panahi I, Chung KM, Horner T, Nadaski M, Chyan J. Design of active noise control systems with the tms320 family. Texas Instruments 1996.
[10] Kuo SM, Morgan DR. Active noise control: a tutorial review. Proc IEEE 1999;87(6):943–73. https://doi.org/10.1109/5.763310
[11] Zhang S, Zhang L, Meng D, Pi X. Active control of vehicle interior engine noise using a multi-channel delayed adaptive notch algorithm based on FxLMS structure. Mech Syst Signal Process 2023;186:109831. https://doi.org/10.1016/j.ymssp.2022.109831
[12] Chen W, Liu Z, Hu L, Li X, Sun Y, Cheng C, et al. A low-complexity multichannel active noise control system using local secondary path estimation and clustered control strategy for vehicle interior engine noise. Mech Syst Signal Process 2023;204:110786. https://doi.org/10.1016/j.ymssp.2023.110786
[13] Ferrari CL, Cheer J, Mautone M. Investigation of an engine order noise cancellation system in a super sports Car. Acta Acust 2023;7:1. https://doi.org/10.1051/aacus/2022060
[14] Elliott SJ. A review of active noise and vibration control in road vehicles. Technical Report University of Southampton; 2008; 981.
[15] Samarasinghe PN, Zhang W, Abhayapala TD. Recent advances in active noise control inside automobile cabins: toward quieter cars. IEEE Signal Proc Mag 2016;33(6):61–73. https://doi.org/10.1109/MSP.2016.2601942
[16] Yoshida T. Active noise control for tractor operator. Jpn Agric Res Q 1995;29(3):161–70.
[17] Pochi D, Fanigliulo R, Del Duca L, Nataletti P, Vassalini G, Fornaciari L, et al. First investigation on the applicability of an active noise control system on a tracked tractor without cab. J Agric Eng 2013;44(s2). https://doi.org/10.4081/jae.2013.394
[18] Carme C, Fohr F, Besombes M. Active noise reduction in the cabin of an earth-moving machine. Proc Of ACTIVE 2002;1:285–90.
[19] Gulyas K, Pinte G, Augusztinovicz F, Desmet W, Sas P. Active noise control in agricultural machines. Proc ISMA 2002;1:11–22.
[20] Sun M, Lu C, Liu Z, Chen W, Shen C, Chen H. A new feedforward and feedback hybrid active noise control system for excavator interior noise. Appl Acoust 2022;197:108872. https://doi.org/10.1016/j.apacoust.2022.108872
[21] Fanigliulo R, Del Duca L, Fornaciari L, Grilli R, Tomasone R, Pochi D. Efficiency of an anc system in the tractor cabin under controlled engine workload. Noise Control Eng J 2020;68(5):339–57. https://doi.org/10.3397/1/376829
[22] Fornaciari L, Del Duca L, Pochi D, Grilli R, Biocca M, Bassotti B, et al. Investigation on the applicability of an active noise control system in the tractor cabin under controlled workload conditions. In: International conference on safety, health and welfare in agriculture and agro-food systems; vol. 521. 2023. p. 38–48. https://doi.org/10.1007/978-3-031-63504-5_5
[23] Paurobally R, Pan J. Practical active noise control - results and difficulties. Proc Of ICSV12 2005;1:1–8.
[24] Pan J, Paurobally R, Qiu X. Active noise control in workplaces. Acoust Aust 2016;44:45–50. https://doi.org/10.1016/j.ymssp.2023.110940
[25] Oh SH, Kim HS, Park Y. Active control of road booming noise in automotive interiors. J Acoust Soc Am 2002;111(1):180–8. https://doi.org/10.1121/1.1420390
[26] Cheer J, Elliott SJ. The design and performance of feedback controllers for the attenuation of road noise in vehicles. Int J Acoust Vib 2014;19(3):155–64. https://doi.org/10.1121/1.1420390
[27] Zafeiropoulos N, Ballatore M, Moorhouse A, Mackay A. Active control of structure-borne road noise based on the separation of front and rear structural road noise related dynamics. SAE Int J Passeng Cars - Mech Syst 2015;8(3):886–91. https://doi.org/10.4271/2015-01-2222
[28] Zhang L, Meng D, Zhang S. Active control of vehicle interior road noise using nfxlms algorithm with two loudspeakers. Proc ICSV26 2019;1:538–45.
[29] Jia Z, Zheng X, Zhou Q, Hao Z, Qiu Y. A hybrid active noise control system for the attenuation of road noise inside a vehicle cabin. Sensors 2020;20(24):7190. https://doi.org/10.3390/s20247190
[30] Kim S, Altinsoy ME. Active control of road noise considering the vibro-acoustic transfer path of a passenger Car. Appl Acoust 2022;192:108741. https://doi.org/10.1016/j.apacoust.2022.108741

[31] Misol M, Algermissen S, Monner HP. Experimental investigation of different active noise control concepts applied to a passenger Car equipped with an active windshield. J Sound Vib 2012;331(10):2209–19. https://doi.org/10.1016/j.jsv.2012.01.001

[32] Mori F, Santoni A, Fausti P, Pompoli F, Bonfiglio P, Nataletti P. The effectiveness of least mean squared-based adaptive algorithms for active noise control system in a small confined space. Appl Sci 2023;13(20):11173. https://doi.org/10.3390/app132011173

[33] Zhou Y, Zhang Q, Yin Y. Active control of impulsive noise with symmetric α-stable distribution based on an improved step-size normalized adaptive algorithm. Mech Syst Signal Process 2015;56-57:320–39. https://doi.org/10.1016/j.ymssp.2014.10.002

[34] Narasimhan SV, Veena S, Lokesha H. Variable step-size griffiths' algorithm for improved performance of feedforward/feedback active noise control. Signal Image Video Process 2010;4(3):309–17. https://doi.org/10.1007/s11760-009-0120-9

[35] Bismor D, Czyz K, Ogonowski Z. Review and comparison of variable step-size lms algorithms. Int J Acoust Vibr 2016;21(1):24–39. https://doi.org/10.20855/ijav.2016.21.1392

[36] Oh JY, Jung HW, Lee MH, Lee KH, Kang YJ. Enhancing active noise control of road noise using deep neural network to update secondary path estimate in real time. Mech Syst Signal Process 2024;206(1):110940. https://doi.org/10.1016/j.ymssp.2023.110940

[37] Akhtar MT, Abe M, Kawamata M. A method for online secondary path modeling in active noise control systems. In: ieee international symposium on circuits and systems; vol. 1. 2005. p. 264–7. https://doi.org/10.1109/ISCAS.2005.1464575

[38] Akhtar MT, Abe M, Kawamata M, Mitsuhashi W. A simplified method for online acoustic feedback path modeling in multichannel active noise control systems. In: sice annual conference; 2008. p. 50–4. https://doi.org/10.1109/SICE.2008.4654621